Developmental Biology 318 (2008) 335–346

Contents lists available at ScienceDirect

Developmental Biology

journal homepage: www.elsevier.com/developmentalbiology

Protocadherin-18a has a role in cell adhesion, behavior and migration in zebrafish development

Emil Aamar, Igor B. Dawid *

Laboratory of Molecular Genetics, Eunice Kennedy Shriver National Institute of Child Health and Human Development, National Institutes of Health, Building 6B, Room 413, Bethesda, MD, USA

ARTICLE INFO

Article history:
Received for publication 21 November 2007
Revised 21 March 2008
Accepted 26 March 2008
Available online 9 April 2008

Keywords:
Adhesion
Migration
Protocadherin
Gastrulation
Hatching gland
Cell dissociation

ABSTRACT

Protocadherin-18a (Pcdh18a) belongs to the δ2-protocadherins, which constitute the largest subgroup within the cadherin superfamily. Here we present isolation of a full-length zebrafish cDNA that encodes a protein highly similar to human and mouse Pcdh18. Zebrafish *pcdh18a* is expressed in a complex and dynamic pattern in the nervous system from gastrula stages onward, with lesser expression in mesodermal derivatives. Pcdh18a-eGFP fusion protein is expressed in a punctate manner on the membranes between cells. Overexpression of *pcdh18a* in embryos caused cyclopia, mislocalization of hatching gland tissue, and duplication or splitting of the neural tube. Most neural markers tested were expressed in an approximately correct A–P pattern. By cell transplantation we showed that overexpression of *pcdh18a* causes diminished cell migration and reduced cell protrusions, resulting in a tendency of cells to stay more firmly aggregated, probably due to increased cell adhesion. In contrast, knockdown of *pcdh18a* by a morpholino oligonucleotide caused defects in epiboly, and led to reduced cell adhesion as shown by cell dissociation, sorting and transplantation experiments. These results suggest a role for Pcdh18a in cell adhesion, migration and behavior but not cell specification during gastrula and segmentation stages of development.

Introduction

Cadherins constitute a superfamily of calcium-dependent cell–cell adhesion glycoproteins, which are present in vertebrates and invertebrates. Cadherins play essential roles in selective cell–cell interactions, and their function is critical during vertebrate embryogenesis and in the adult CNS (Hirano et al., 2003; Redies, 2000; Takeichi, 1991; Vleminckx and Kemler, 1999; Zou et al., 2007). Approximately 100 diverse cadherin superfamily genes are expressed in the brain (Hamada and Yagi, 2001; Kaneko et al., 2006; Yagi and Takeichi, 2000). Cadherins are involved in many biological processes, including cell recognition, signaling and communication during embryogenesis, formation of neural circuits, morphogenesis, angiogenesis, maintenance of cell structure, and possibly neurotransmission (Angst et al., 2001; Bel and Escriche, 2006; Morishita et al., 2006; Takeichi, 1988; Tepass et al., 2000; Wheelock and Johnson, 2003; Yagi and Takeichi, 2000).

The cadherin superfamily can be divided into at least six categories according to their structural and functional properties: classic cadherins (types I and II), desmosomal cadherins, and a large group of atypical cadherins which includes the flamingo, FAT, T-cadherin, and protocadherin (pcdh) families (Angst et al., 2001; Bekirov et al., 2002; Bel and Escriche, 2006; Morishita et al., 2006; Nollet et al., 2000; Uemura, 1998; Zou et al., 2007). With 80 members, the pcdhs (Sano et al., 1993) represent the largest subclass of the non-classical cadherins (Frank and Kemler, 2002; Nollet et al., 2000; Patel et al., 2003; Reiss et al., 2006; Shapiro and Colman, 1999; Suzuki, 2000). Pcdhs contain six or more extracellular cadherin repeats, a single transmembrane domain, and diverse cytoplasmic regions that do not interact directly with β-catenin as classical cadherins do (Cronin and Capehart, 2007; Gooding et al., 2004; Yoshida et al., 1999). Several subfamilies of pcdhs have been identified, such as the α, β, γ and δ-pcdhs, and the large pcdhs (Fat- and Dachsous-related) (Frank and Kemler, 2002; Hirano et al., 2003; Vanhalst et al., 2005). Nine human pcdhs (PCDH1, -7, -8, -9, -10, -11, -17, -18, and -19) and their mouse orthologues are grouped into the δ-pcdh class, although their mutual homology is moderate. This subfamily is characterized by two motifs in their cytoplasmic domains, the highly conserved CM1 and the less conserved but identifiable CM2 domain (Redies et al., 2005; Vanhalst et al., 2005; Wolverton and Lalande, 2001).

The δ-pcdhs can be further subdivided in two subgroups, δ1 and δ2, on the basis of overall homology, number of extracellular cadherin repeats (seven *versus* six), and conservation of specific amino acid motifs in the cytoplasmic domains. The δ1 subgroup comprises Pcdh1, -7, -9, and -11 or X/Y while the δ2 subgroup comprises Pcdh8, -10, -17, -18, and -19 (Redies et al., 2005; Vanhalst et al., 2005). δ1-pcdhs contain a short motif (RRVTF: CM3) in their cytoplasmic domain, which is necessary for the binding between human PCDH7 and protein phosphatase-1α (PP1-α) (Redies et al., 2005; Vanhalst et al., 2005; Yoshida et al., 1999), a cytosolic phosphatase believed to be

* Corresponding author.
E-mail address: idawid@nih.gov (I.B. Dawid).

0012-1606/$ – see front matter © 2008 Published by Elsevier Inc.
doi:10.1016/j.ydbio.2008.03.040

important in synaptic plasticity (Munton et al., 2004). Mouse Pcdh18, a δ2-pcdh, interacts with Disabled-1 (Homayouni et al., 2001; Redies et al., 2005), a protein involved in the Reelin pathway and needed for correct formation of cortical neuron layers (Howell et al., 1999, 2000).

Little is known about the function of pcdhs in cell adhesion or development. Some δ-pcdhs were reported to mediate weak cell–cell adhesion in vitro and have a role in cell sorting in vivo. In particular, in vitro adhesive activity has been demonstrated for Pcdh1 (Sano et al., 1993), Pcdh7 (Yoshida, 2003), Pcdh8 (Yamagata et al., 1999) and Pcdh10 (Hirano et al., 1999). Moreover, by preferring homophilic over heterophilic interactions, some δ-pcdhs are able to mediate cell sorting in cell culture (e.g. Pcdh1 (Sano et al., 1993) and Pcdh10 (Hirano et al., 1999)) and in vivo. Axial pcdh (AXPC, the presumed Pcdh1 ortholog) and paraxial pcdh (PAPC, related to Pcdh8) mediate sorting of paraxial and pre-notochordal mesenchyme during *Xenopus* gastrulation (Kim et al., 1998; Kuroda et al., 2002). PAPC affects adhesion indirectly by regulating the activity of C-cadherin (Chen and Gumbiner, 2006). This was also supported by the finding that arcadlin/PAPC regulates the activity of N-cadherin in synaptic membranes by triggering its endocytosis (Yasuda et al., 2007). NF-pcdh, the presumed Pcdh7 ortholog, can mediate cell sorting in the embryonic epidermis of *Xenopus* in a homotypic manner, but not in the absence of its intracellular domain (Bradley et al., 1998). In addition, individual δ-pcdhs might play a role in signaling pathways as they bind to proteins such as TAF1/Set, PP1-α and Frizzled 7 (Homayouni et al., 2001; Redies et al., 2005).

Although Pcdh18 was described in mice, not much is known about its role in embryonic development. Mouse Pcdh18 is present throughout the embryo, in particular in the ventricular zone in the forebrain and midbrain, in the olfactory bulb, cerebral cortex, thalamus, cerebellum, and in additional organs of the adult (Homayouni et al., 2001; Wolverton and Lalande, 2001). In the present work, we report the isolation of the *pcdh18a* gene from zebrafish and the characterization of its expression and function during embryonic development. We show that overexpression or suppression of expression of Pcdh18a results in embryonic malformations characterized by deficits in cell behavior and cell movement. Based on cell dissociation, sorting and transplantation experiments we suggest that Pcdh18a functions in promoting cell–cell adhesion in the zebrafish embryo.

Materials and methods

Embryos

Zebrafish (*Danio rerio*) were raised and maintained according to standard procedure (Westerfield, 2000). Embryos were raised at 28.5 °C and staged as described (Kimmel et al., 1995).

RT-PCR

RNA isolation was performed using the RNeasy Mini Kit (Qiagen, http://www1.qiagen.com). Reverse transcription and PCR were performed as described in the SuperScript™ II Reverse Transcriptase manual (Invitrogen, http://www.invitrogen.com). The expression levels of *pcdh18* were compared to those of a house keeping gene *histone 4* (*H4*, AM422106). The primers used for *H4* were: forward, 5′-GAAGAGG-CAAAGGAAGCAAA-3′ and reverse, 5′-TGGCGTGCTCTGTGTAGGTA-3′ (58 °C, 25 cycles). The primers used for *pcdh18a* were: forward, 5′-CAGCTCACAGCCTCAGACAG-3′ and reverse, 5′-ATTTTCCCATTGGTCCCTTC-3′ (58 °C, 30 cycles).

Cloning and construction of expression plasmid

A partial zebrafish *pcdh18a* clone (#5114) was identified in an expression pattern screen (Kudoh et al., 2001). The 5′ end of *pcdh18a* was subsequently generated by 5′-RACE using the SMART RACE Kit (Clontech) with a gene-specific primer (5′-ACCTG-TAGATGACGCCTTACCCGGTAG-3′), and sequenced. Full-length ORF cDNA was then RT-PCR amplified and subcloned into the EcorI–-XhoI sites of the expression vector pCS2+ (Turner and Weintraub, 1994). Pcdh18a-eGFP fusion protein was prepared by replacing the stop codon in pcdh18a with a ClaI site which is also found upstream (5′ end) of the eGFP construct. The EcoRI–Cla1 *pcdh18a* fragment was ligated to the 5′ end of eGFP maintaining the reading frame, and subcloned into pCS2+.

Whole-mount in situ hybridization

In situ hybridizations were performed as described by Thisse and Thisse (http://zfin.org/zf_info/zfbook/chapt9/9.82.html) (Westerfield, 2000). Antisense digoxigenin-labeled probes were synthesized for the zebrafish *dlx3* (edge of the neural plate) (Akimenko et al., 1994), *ctsl1b/hgg1* (polster or hatching gland) (Andreas and Vogel, 1997; Thisse et al., 1994), *ntl* (notochord) (Schulte-Merker et al., 1994), *egr2/krox20* (rhombomeres 3 and 5) (Oxtoby and Jowett, 1993), *pax2a* (hindbrain, midbrain hindbrain boundary, optic stalk, pronephric duct, spinal cord) (Krauss et al., 1991; Pfeffer et al., 1998), *floating-head* (*flh*) (Melby et al., 1997), *wnt1* (midbrain, midbrain hindbrain boundary, roof plate rhombomeres 2–8) (Molven et al., 1991), *engrailed2* (*eng2*) (midbrain hindbrain boundary) (Fjose et al., 1992), *fgf8* (midbrain hindbrain boundary) (Furthauer et al., 1997; Reifers et al., 1998) and other markers not shown. The labeling kit from Roche Molecular Biochemicals was used as described (Westerfield, 2000).

RNAs and morpholinos

Pcdh18a, *pcdh18a-eGFP*, membrane-bound *RFP* (*mRFP*), *GFP* and membrane-bound *GFP* (*mGFP*) mRNAs were prepared using clones linearized with NotI and transcribed using the mMESSAGE mMACHINE® SP6 Kit (Ambion). Morpholino antisense oligonucleotides (Gene Tools) were as follows: *pcdh18a* ATG-MO (translation blocking morpholino), 5′-GCACTGTACCCTTGCTGGTCTCCAT-3′ (bases complementary to the predicted start codon are indicated in italics and underlined); *pcdh18a* 5′ UTR-MO, 5′-TCCGTCAGGCACTGCAAAAATATAC-3′ which aligns to the regions from -8 to -32 upstream to the ATG site; and Gene Tools standard control MO.

Cell transplantation

For cell transplantations, donor embryos were injected with 5 ng rhodamine–dextran (fluoro-ruby, MW 10,000, Molecular probe, Invitrogen) plus 150–200 pg *pcdh18a* RNA, or with 5 ng fluorescein–dextran (fluoro-emerald, MW 10,000, Molecular probe, Invitrogen) plus 150–200 pg *GFP*. Cells were taken from sphere or 40% stage donor embryos and transplanted into animal or marginal regions of same stage host wild-type embryos. The technique was modified from that previously described by Heisenberg et al. (2000). Photographs were taken for 80–90% epiboly live or fixed embryos under dissecting or confocal microscopes with regular light, UV illumination or laser screening.

Analyses of sub-cellular protein localization

To monitor Pcdh18a localization, embryos at the one-cell stage were injected with 150 pg RNA encoding *pcdh18a-eGFP* alone, or combined with 25 pg *mRFP* RNA (membrane-bound red fluorescent protein, gift from N. Ueno (Iioka et al., 2004)), and were mounted in 1% agar in embryo medium at 80–90% epiboly (Westerfield, 2000). Image analysis of live embryos was carried out using a Zeiss LSM 510 Meta confocal microscope with a 63× water-immersion lens. Alternatively the injected embryos were fixed and mounted in glycerol before examining them by confocal microscopy.

Dissociation assay

The method was modified from that used for dissociating *Xenopus* animal caps. Embryos were injected at the one-cell stage with *mGFP* RNA, *pcdh18a* RNA, control MO (CO-MO), or pcdh18a 5′ UTR-MO alone or combined with *pcdh18a* RNA. At the high stage, embryos were dechorionated by Pronase treatment, washed several times with egg water, and kept in embryo medium (Westerfield, 2000) until sphere stage. At sphere-dome stage blastoderms were dissected and separated from the yolk using fine forceps, and moved to a 12-well plastic plate containing 1% agarose in calcium–magnesium free medium (CMFM; 88 mM NaCl, 1 mM KCl, 7.5 mM Tris pH 7.6, 2.4 mM $NaHCO_3$, 0.1 mM EDTA (Gurdon et al., 1984; Sargent et al., 1986). At the beginning the wells contained 1 ml of high-calcium Ringer's solution (Westerfield, 2000), in which the explants were allowed to heal for about 5–10 min. The solution was then replaced by 1 ml CMFM and dissociation of the explants was monitored while vertically rotating the plate at 50–75 rpm.

Cell sorting assay

Embryos were injected at the one-cell stage with fluoro-emerald dextran alone or in combination with *pcdh18a* RNA, or injected with ruby red dextran alone or in combination with pcdh18a 5′ UTR-MO. At the high stage, embryos were dechorionated by Pronase treatment, washed, and cultured until sphere stage. Fifteen emerald (green) and 45 ruby red (red) labeled embryos were combined in one 1.7 ml plastic tube, for control or experimental samples. One milliliter of calcium free Ringer's solution with EDTA (Westerfield, 2000) was added to each of the samples, which were dissociated by gently inverting the tubes and pipetting; embryos dissociate into single cells within 2–5 min. The cells were centrifuged at 500 rpm for 3 min, re-suspended in 0.5 ml Ringer's solution, and moved to 35×10 mm agar-coated culture dish containing 2.5 ml high-calcium Ringer's solution (Westerfield, 2000). Reaggregation proceeded with rotation at 50 rpm, with progress documented by fluorescent photography up to 4 h.

Imaging

Live, fixed, or in situ stained embryos were observed and photographed by using a Leica MZ APO dissecting microscope with a RETIGA 1300 digital camera (Quantitative Imaging Corporation) using the QCapture software. Fluorescence was observed in a Leica DFC500 camera (on Leica MZ16F) or in a Leica MZ FLIII fluorescence stereomicroscope and the Diagnostic Instruments Corp. spot digital camera RT slider system and software version 4.5. Confocal micrographs were taken using the Zeiss LSM 510 Meta axioplan2 Laser Scanning Microscope.

Sequence homology, alignments and structure analysis

For sequence comparisons and alignments we used the following programs: http://www.ncbi.nlm.nih.gov/BLAST/, http://align.genome.jp/, and http://smart.embl-heidelberg.de/.

Results

Sequence and structure of zfpcdh18a

Our studies of Pcdh18a started with cDNA clone 5114 (Gene Bank BG985781) isolated in our gene expression screen (Kudoh et al., 2001), which was extended by 5′-RACE. The full sequence was submitted to GenBank under accession number EU267178. The ORF obtained from this analysis predicts a protein that shares 65–66% identity with Pcdh18 in *Xenopus tropicalis*, mouse, rat and human (Fig. 1A; Supplementary Fig. 1), and displays a domain structure characteristic of pcdhs (see below). Recently, NCBI listed a closely similar sequence as an unidentified predicted zebrafish gene or protein under XM_696257, LOC572532 and XP_701349. The minor differences between our Pcdh18a sequence and that listed under XP_701349 may be due to polymorphisms. While this manuscript was under review, another zebrafish sequence named protocadherin 18 was released (AB297803), with an expression pattern paper in press (Kubota et al., 2008). Mammalian Pcdh18 is the sequence most similar to the protein described here and to that described by Kubota et al., but the two proteins share only 70% sequence identity (Fig. 1A; Supplementary Fig. 1). Further, the expression patterns are quite different. Thus the two proteins may be distinct paralogs of Pcdh18, and following advice from the ZFIN nomenclature committee we name our protein Pcdh18a.

Zfpcdh18 is similar in structure to other members of the δ2-pcdh subfamily, including an extracellular region containing a signal peptide and six cadherin repeats, a single transmembrane region, and an intracellular/cytoplasmic region including the conserved motifs CM1 and CM2 (Redies et al., 2005) (Fig. 1B). By comparing zebrafish to mouse Pcdh18 (Homayouni et al., 2001), conserved SH3 and Disabled-1 binding motifs were found within the intracellular region (Kohmura et al., 1998). PXXP (PKKP in zfpcdh18a) is the minimal consensus sequence for SH3-binding sites (Kohmura et al., 1998), while FQNP has been shown to be a Disabled-1 binding motif in mouse Pcdh18. The cadherin repeats in zfpcdh18a contain the highly conserved amino acid motifs DxD, DRE/DxE, and DxNDNxPxF, which were previously shown to bind to Ca2+ in the classical cadherins (Kohmura et al., 1998; Nagar et al., 1996; Shapiro et al., 1995). As in typical *pcdhs* (Wu and Maniatis, 2000), the *zfpcdh18a* gene is comprised of four exons. The first exon is the largest, encoding the extracellular and transmembrane domains and part of the intracellular region. The second exon is very short followed by a third exon including the CM1 domain and a fourth including the CM2 domain (Fig. 1B).

In order to examine the cellular localization of Pcdh18a, mRNA encoding a fusion protein of zfpcdh18a and eGFP was injected into one-cell stage embryos. Embryos at 80% epiboly stage were examined by confocal microscopy (Fig. 1C), showing that Pcdh18a-eGFP was expressed in a punctate manner along the membranes of adjacent cells, confirming the expected localization of the protein and suggesting a role for Pcdh18a in cell adhesion.

Pcdh18a expression in zebrafish embryos

Pcdh18a mRNA is not present in maternal RNA, can be detected by RT-PCR beginning at the late blastula stage, and increases thereafter (Fig. 2A). By in situ hybridization, the pattern of expression of this gene is complex and dynamic from gastrula stages onward (Figs. 2B–O, Supplementary Fig. 2). *Zfpcdh18a* starts being expressed at the shield stage in the epiblast (Figs. 2B, C), and cells expressing this gene appear to expand in a rostral direction (Figs. 2C–E). At the bud and early somite stages *zfpcdh18a* is expressed in the prechordal plate and

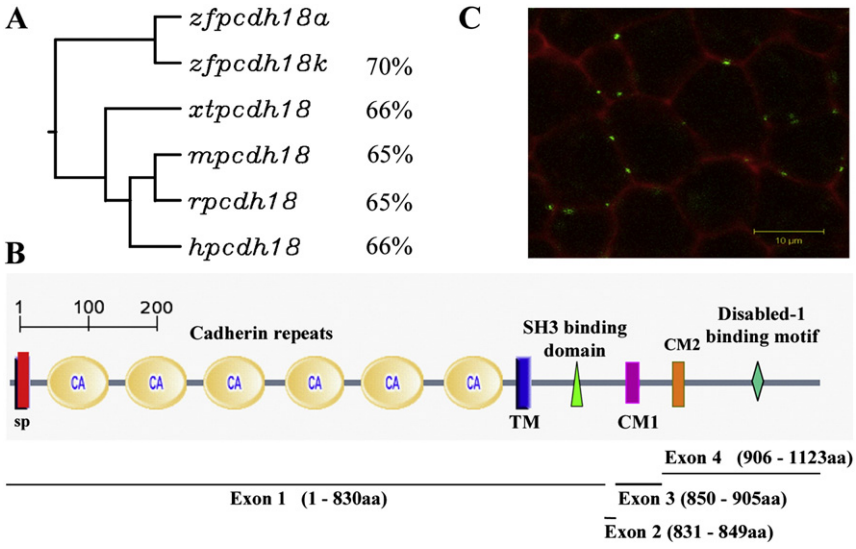

Fig. 1. Pcdh18 family homology, predicted structure and localization. (A) The closest relative to the protein we describe, Pcdh18a (ABX64360), is the protein described by (Kubota et al., 2008), labeled Pcdh18k (BAF96395). Both are related to Pcdh18 in *Mus musculus* (m, AAL47095, 65%), *Homo sapiens* (h, AAH93815, 66%), *Xenopus tropicalis* (xt, NP_001011150, 66%) and *Rattus norvegicus* (r, XP_227117, 65%). (B) Predicted protein structure of zebrafish Pcdh18a. SP, signal peptide sequence (1–29aa); CA1–CA6, six cadherin repeats in the extracellular region (30–701aa); TM, transmembrane region (702–724aa); the cytoplasmic tail (725–1123aa) contains two conserved motifs, CM1 (858–888aa) and CM2 (909–926aa), an SH3 binding motif (755–758aa) and a Disabled-1 binding motif (1044–1047aa). Below is shown the exon/intron arrangement of zfpcdh18a, containing four exons as is typical of pcdhs. (C) Confocal image of a zebrafish embryo at 80% epiboly injected at the one-cell stage with membrane-bound red fluorescent protein (mRFP, red) and pcdh18a-eGFP fusion construct (green). The fusion protein is expressed in a punctate manner at the membranes between cells. The scale is 10 μm.

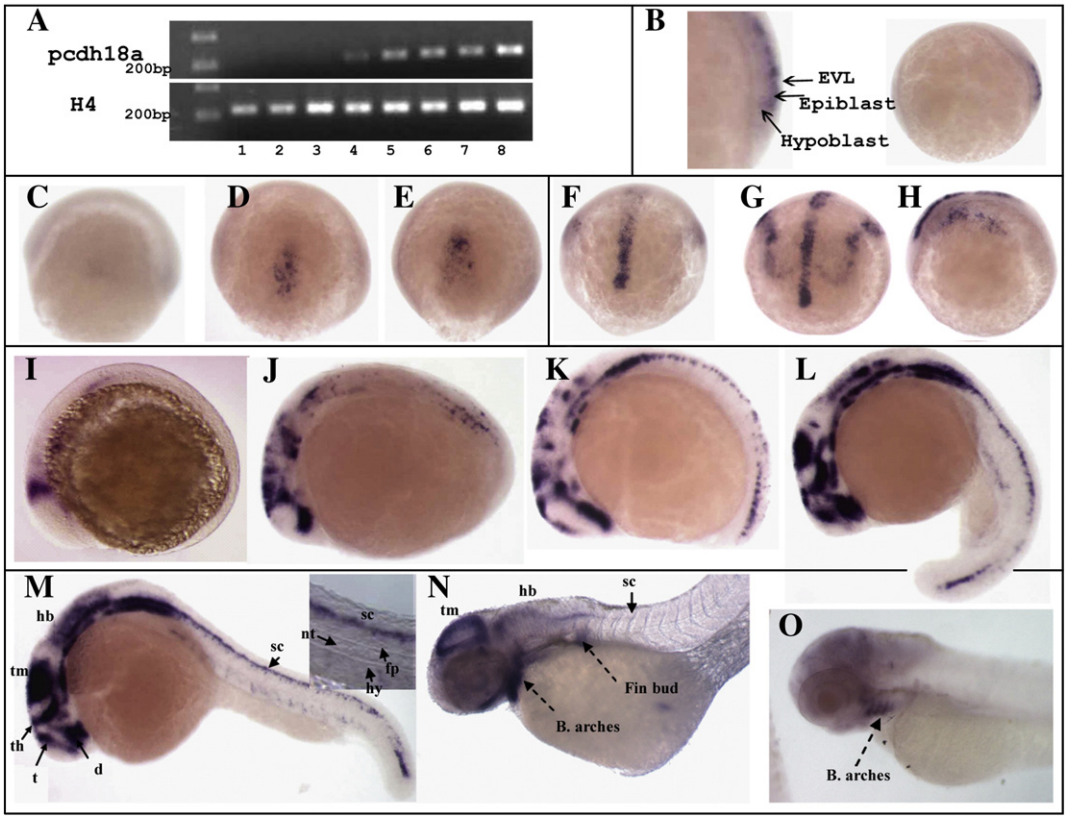

Fig. 2. *Pcdh18a* expression in zebrafish embryos. (A) RT-PCR reactions for *pcdh18a* and *histone 4* (*H4*) as control were performed for different stages (1–8: unfertilized eggs, 100–200 cells, high dome, 40–50% epiboly, 80–90%, bud, 6 somites, and 24 h embryos, respectively). *Pcdh18a* is expressed zygotically but not maternally. (B–O) In situ hybridization for *pcdh18a*. (B) *Pcdh18a* is expressed in the epiblast at about 60% epiboly (lateral view). (C–E) Dorsal views of shield (C), 60% (D) and 90% (E) epiboly stages. (F, G) Anterior views and (H) lateral view of bud (F) and 1 somite stage (G, H), showing lateral expression in addition to the midline expression that arose earlier. (I–L) Lateral views of 2 somite (I), 6 somite (J), 13–14 somite (K), and 18 somite (L) stages. Expression is detected in midbrain, diencephalon, telencephalon, thalamus, hindbrain, spinal cord, otic vesicles and branchial arches. (M) 24hpf embryo; inset, higher magnification of the tail showing expression in spinal cord but not notochord, hypochord or floor plate. (N) 2-day and (O) 3-day old embryos, showing reduced expression that becomes restricted to the branchial arches. B, branchial; hb, Hindbrain; sc, spinal cord; th, thalamus; tm, tectum; d, diencephalon; t, telencephalon; ov, otic vesicles; nt, notochord; hy, hypochord; fp, floor plate.

dorsal midline, and in regions at the lateral edge of the neural plate, possibly corresponding to the neural crest (Figs. 2F–H; note that F and G are anterior views). From mid-somitogenesis to 24hpf *zfpcdh18a* is widely expressed in a dynamic pattern, most extensively in the CNS, including in the diencephalon, telencephalon, thalamus, tectum, hindbrain, otic vesicles and spinal cord (Figs. 2I–M). Other expression domains include the branchial arches and fin buds. The expression at 2 and 3 days of development (Figs. 2N, O) becomes more restricted to the branchial arches and the fin buds, and then the expression fades away.

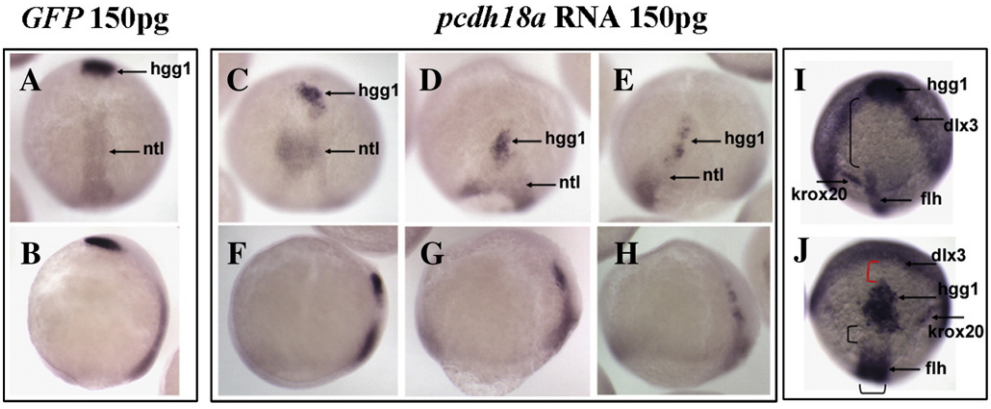

Fig. 3. Pcdh18a overexpression affects cell movements. Embryos injected with *pcdh18a* RNA showed delayed epiboly and impaired cell movements. (A–H) In situ hybridization with *ntl* plus *hgg1* in embryos injected with 150 pg *GFP* RNA (A, B), or 150 pg *pcdh18a* RNA (C–H, three examples shown). In one of several similar experiments, as 95% ($n=37$) of control embryos reached 95% epiboly, the *pcdh18a*-injected embryos were at about 80% epiboly, had shorter and wider *ntl* domains, and *hgg1*-positive cells did not advance normally (60% of embryos, $n=57$). (A, C–E) are dorsal views, (B, F–H) are lateral views. (I, J) Anterior views with dorsal to bottom, showing in situ hybridization using probes for *hgg1*, *flh*, *krox20* and *dlx3* for *GFP* (I), or *pcdh18a* RNA-injected embryos (J); control embryos were at bud stage. The anterior migration of *hgg1*-positive cells is delayed, leading to a gap (red parenthesis in panel J) between the *hgg1* and *dlx3* domains, while the distance from the *hgg1* domain to the *krox20* and *flh* domains is reduced (black parenthesis).

Zfpcdh18a overexpression leads to gastrulation and epiboly defects, shortened axis, mislocalization of the hatching gland, axis duplication, and cyclopia

To evaluate the role of Pcdh18a in development, *zfpcdh18a* or *GFP* RNA as control was injected at the one-cell stage, and embryos were examined at different stages for phenotypic effects. At least 50% of the *zfpcdh18a*-injected embryos showed a delay in epiboly. In one experiment, at a time when 66% of embryos injected with 150 pg *GFP* RNA had reached 60–70% epiboly and 34% were at 40–50% epiboly (n=35), only 9% of embryos injected with 150 pg *pcdh18a* RNA were at 60–70% epiboly, 70% were at 30–40%, and 21% at dome stage (n=23). Cell movements during gastrulation were also compromised resulting in shorter and wider axes, as visualized by in situ hybridization with several marker genes. At the late gastrula stage, the notochord anlage stained by *ntl* was short and wide, and cells expressing *hgg1* (specific marker for polster or hatching gland the most anterior region of the prechordal plate) had advanced less towards the anterior in *pcdh18a* RNA-injected embryos than in control embryos (Figs. 3A–H). The relative positions at the bud stage of the prechordal plate marker *hgg1*, notochord marker *flh*, *dlx3* marking the neural plate boundary and *krox20* which at this stage marks rhombomere 3 also showed that axis elongation was reduced in *pcdh18a* RNA-injected embryos (Figs. 3I, J).

In spite of defects in axis elongation, zebrafish embryos injected with *zfpcdh18a* RNA showed essentially normal expression levels and appropriate relative localization of most markers examined, which included *wnt1*, *wnt8*, *wnt11*, *fgf8*, *dlx2a*, *six3*, *krox20*, *eng2*, *pax6.1*, *shh*, *ntl*, *flh*, *dlx3*, *mbx*, *myod*, *Col2a1*, *gsc*, *huc1*, *pax2a*, *bmp2*, *bmp4*, *chd*, *cyc*, *mkp3*, *sox17* and *sqt*. The most pronounced abnormal

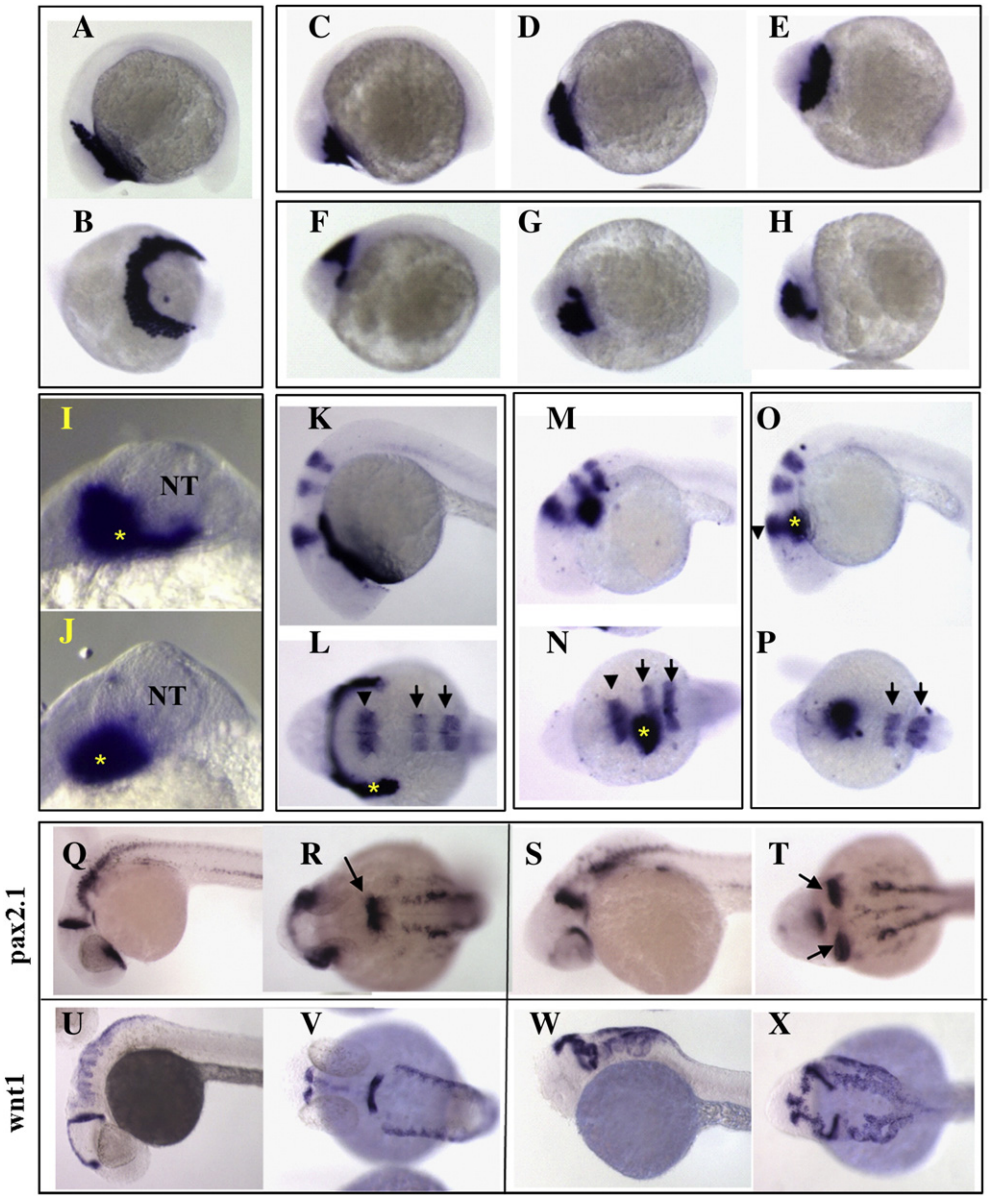

Fig. 4. Hatching gland mislocalization in Pcdh18a-overexpressing embryos. In situ hybridization with *hgg1* on 12-somite stage embryos (A–J) injected with 100 pg *GFP* RNA (A, B) or 100 pg *pcdh18a* RNA (C–J). In two experiments, 13 of 24 (54%) of the *pcdh18a* RNA-injected embryos showed mislocalization of *hgg1*, while none of the *GFP*-injected embryos (n=18) did. (I, J) show two examples of *hgg1* staining (asterisk) in relation to the neural tube (NT), taken at higher magnification in anterior view. (K–P) In situ hybridization with *hgg1* (asterisk), *krox20* (arrow) and *eng2* (arrowhead) at 24hpf, shows mislocalization of *hgg1*-expressing cells, but an almost normal pattern of *krox20* and *eng2* in embryos injected with 100 pg *pcdh18a* RNA (37 of 50, 74%, in three experiments; M–P). None of the 34 *GFP* RNA-injected embryos showed this phenotype (K, L). (Q–X) Neural tube duplications in *pcdh18a* RNA-injected embryos at 28hpf were visualized by in situ hybridization with *pax2.1* (S, T), and *wnt1* (W, X); control embryos are shown in panels Q, R, U, V. Combining data from several experiments using different markers showed duplications in 119 of 202 (59%) injected embryos.

localization was exhibited by *hgg1*, a gene that marks the hatching gland. Cells expressing *hgg1* were strongly inhibited in their migration, becoming surrounded and engulfed by adjacent cells that progress to positions close to their normal location in the embryo. A delay in movement of *hgg1*-expressing cells is already apparent during gastrulation (Fig. 3) and becomes more pronounced during somite stages (Figs. 4A–J). At 24hpf, *hgg1*-expressing cells were located in the mid-hindbrain region in many *pcdh18a*-injected embryos, even though the expression pattern of *eng2* and *krox20* was close to normal (Figs. 4K–P).

In addition to the phenotypes described above, Pcdh18a overexpression also affects the shaping of the neural tube. In addition to having a shorter and wider neural tube, some embryos exhibited apparent duplication or splitting of the neural tube in the mid-hindbrain regions that fused caudally into a single structure. This effect was visualized by in situ hybridization with *pax2.1* (Figs. 4Q–T) and *wnt1* (Figs. 4U–X); use of additional markers including *huc1*, *pax6.1*, *six3*, *eng2* and *krox20* confirmed these observations (not shown; see legend of Fig. 4 for frequency).

Inspection of unstained embryos overexpressing Pcdh18a also showed phenotypes with a range of severity, including shortened and widened body axis, indications of split neural tube, cyclopia, abnormal somites and small and abnormal pharyngeal arches (Supplementary Fig. 3, and data not shown).

These results indicate that Pcdh18a has a role in cell migration but not cell specification during embryonic development, with a pronounced effect on the localization of hatching gland cells. Reduced migrations of *hgg1*-expressing cells, as well as cyclopia are also seen in *slb/wnt11* mutants that are defective in the Wnt/PCP pathway controlling gastrulation movements (Heisenberg et al., 2000; Ulrich et al., 2003).

Knocking down endogenous pcdh18a in zebrafish embryos caused cell migration defects

Embryos injected with a morpholino complementary to a region including the ATG showed a delay in epiboly compared to controls (Figs. 5A, B). At later stages, the injected embryos showed shortened

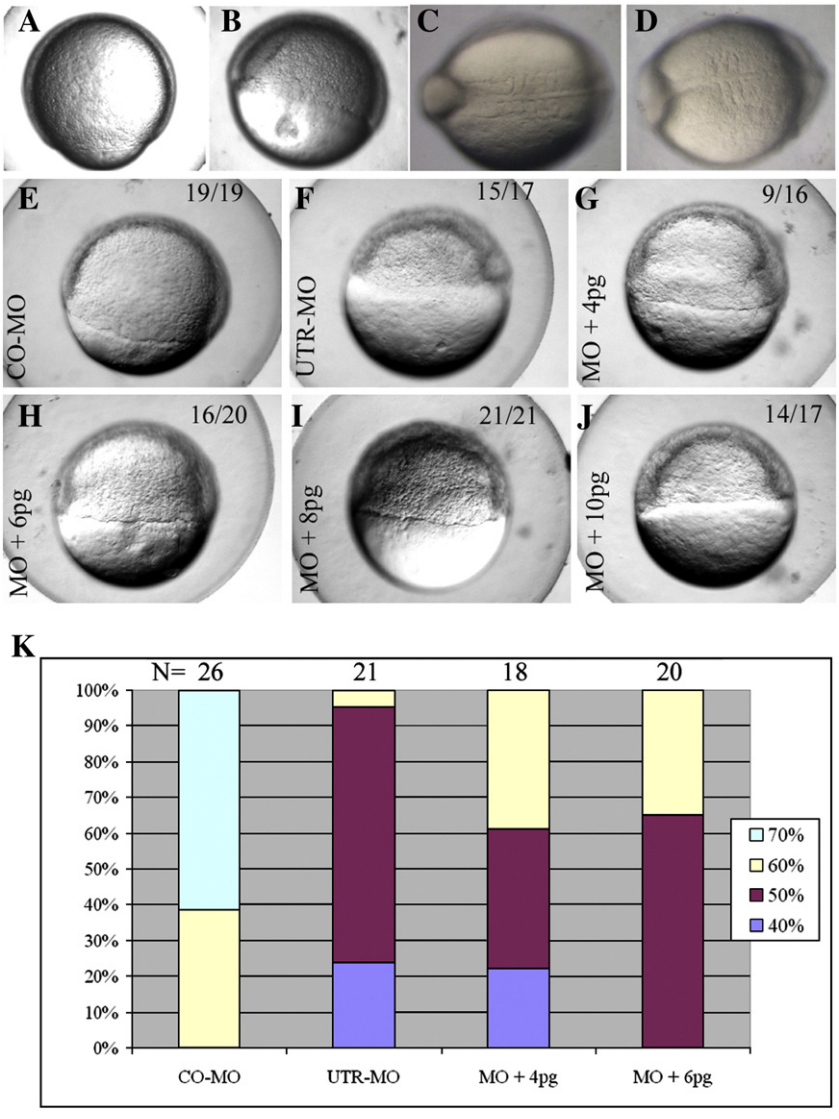

Fig. 5. Impaired development resulting from *pcdh18a* knockdown, and rescue by *pcdh18a* RNA co-injection. CO-MO (A, C) or *pcdh18a* ATG-MO (5 ng) (B, D) were injected into embryos at the one-cell stage. ATG-MO-injected embryos (B) showed delayed epiboly (11 of 17, 74%, in one of five experiments) compared to controls (A). Likewise, as control MO-injected embryos reached the 5 somite stage (C), ATG-MO-injected embryos contained 3–4 somites that were wider than normal (D; 25 of 32, 78%). (E–J) Phenotype caused by UTR-MO and its rescue. UTR-MO (F–J) was injected alone (F) or together with 4, 6, 8, and 10 pg *pcdh18a* RNA (G–J, respectively); CO-MO is in panel E. The UTR-MO-injected embryos showed a delay in epiboly that was rescued by co-injection of the RNA. Quantification of one of four similar experiments is shown in panel K. The color code refers to the percentage of embryos in the respective stage of epiboly at the same time point.

axis with wider somites whose formation was delayed compared to control embryos (Figs. 5C, D). A non-overlapping morpholino targeting the 5′-UTR yielded similar phenotypes (Figs. 5E, F), which supports the specificity of the morpholino action. We have also shown that the ATG-MO inhibits expression of an injected Pcdh18a-GFP fusion construct in the embryo (data not shown). Specificity was further supported by the fact that RNA co-injection substantially rescued the developmental delay produced by the UTR-MO (Figs. 5E–J). Quantification of the rescue of developmental progression during epiboly in one representative experiment among four that were carried out, supports the view that the action of this morpholino is specific (Fig. 5K). Additional evidence for specificity of morpholino action was obtained in cell dissociation assays, as discussed below. Rescue of the epiboly delay phenotypes by RNA co-injection was not complete, likely due to the fact that *pcdh18a* RNA overexpression itself results in abnormal development. It is known that inhibition or overexpression of components that affect cell movements and polarity result in similar phenotypes (Heisenberg et al., 2000; Ulrich et al., 2003). In later development, UTR-MO-injected embryos showed further developmental delay, shortened axis, cell death and dose-dependent embryonic lethality during mid-somitogenesis stages (data not shown). From these experiments we conclude that Pcdh18a is required for early development of the zebrafish embryo.

Pcdh18a strengthens cell adhesion

Since the immediate effect of reduced or excess expression of Pcdh18a in zebrafish embryos was a delay in epiboly and impaired gastrulation movements, we investigated the role of Pcdh18a in cell adhesion by carrying out cell dissociation experiments. For this purpose, embryos were injected with CO-MO (Figs. 6A–E) or UTR-MO alone (Figs. 6F–J), UTR-MO and *pcdh18a* RNA (Figs. 6K–O), *mGFP* RNA as control (Figs. 6P–T), and *pcdh18a* RNA (Figs. 6U–Y). The embryos were raised to the sphere stage, blastoderms were dissected and transferred to calcium–magnesium free medium (CMFM, see Materials and methods). While shaking at 50–75 rpm, the samples were monitored for cell dissociation. Cells from CO-MO and mGFP injected embryos dissociated at the same rate, whereas cells from UTR-MO-

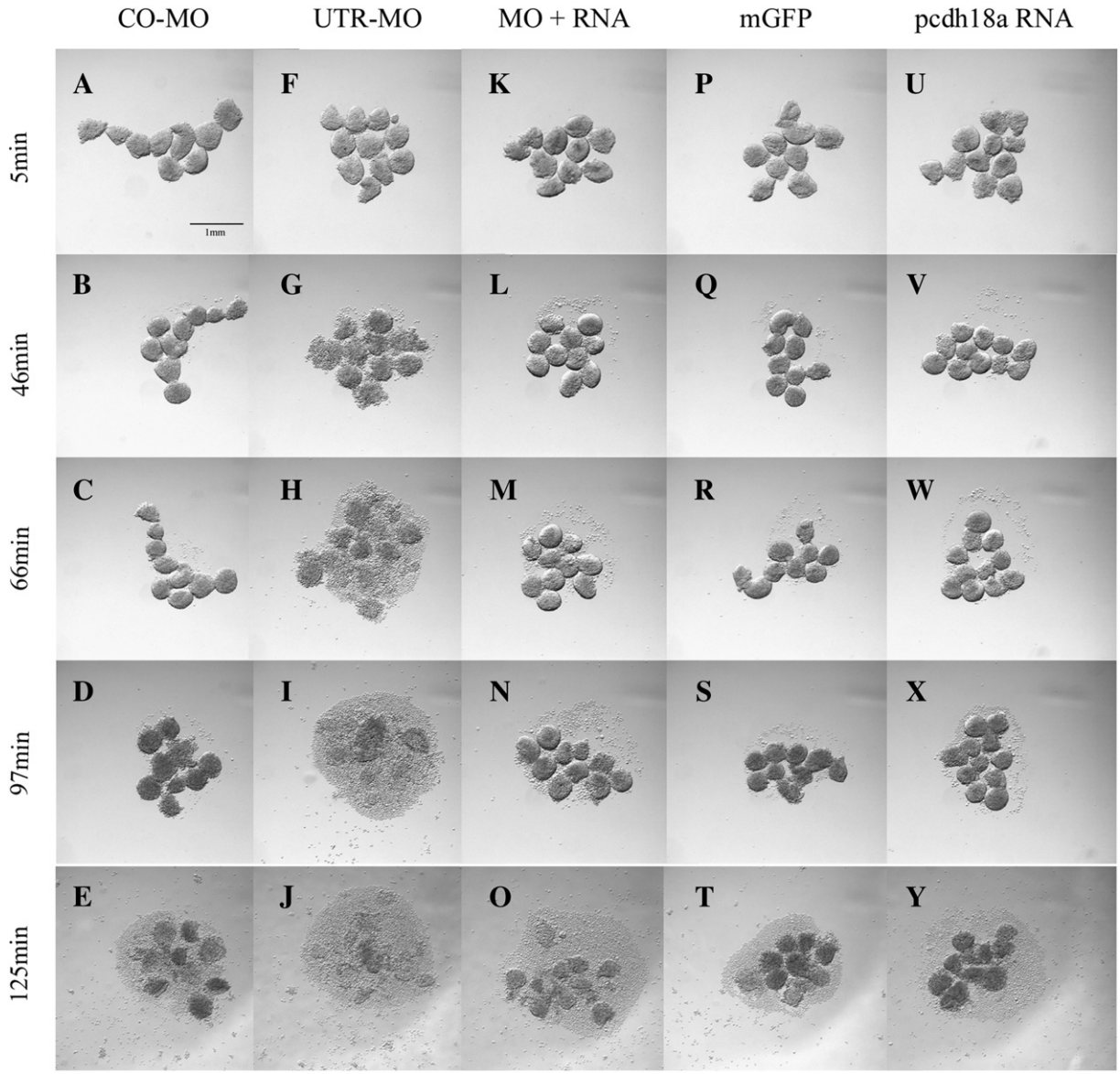

Fig. 6. Pcdh18a affects cell dissociation. Embryos injected with 10 ng CO-MO (A–E), 8 ng *pcdh18a* 5′ UTR-MO (F–J), 250 pg *mGFP* RNA (P–T), 250 pg *pcdh18a* RNA (U–Y), and a combination of 8 ng UTR-MO and 250 pg *pcdh18a* RNA (K–O), were tested for cell dissociation. Blastoderms were dissociated in CMFM with rotation (see Materials and methods), and photographed at the times indicated. The test was repeated three times with consistent results. Scale bar shown in panel A is 1 mm.

injected embryos dissociated faster and more completely (Figs. 6F–J vs. A–E, P–T). Furthermore, co-injection of *pcdh18a* RNA could rescue the fast dissociation caused by the UTR-MO (Figs. 6K–O), restoring a dissociation rate comparable to that of embryos injected with CO-MO or GFP. Injection of *pcdh18a* RNA alone had little effect on the rate of dissociation (Figs. 6U–Y). This experiment was repeated three times with consistent results, indicating that Pcdh18a contributes to the adhesion between embryonic cells in the zebrafish blastula, and providing additional evidence for the specificity of action of the UTR-MO.

These findings were further supported by cell sorting experiments (Fig. 7) which were repeated more than three times. Embryos were injected with fluoro-emerald dextran (green) alone or together with *pcdh18a* RNA, and with ruby red dextran alone or together with pcdh18a 5′ UTR-MO. The embryos were dissociated into single cells at the sphere stage. Red and green control cells or experimental cells were mixed, and allowed to reaggregate (see Materials and methods). Control red and green cells showed uniform distribution in the aggregates (Figs. 7A–C, G, H, K). In contrast, green cells overexpressing *pcdh18a* RNA stayed closer to each other than to red cells injected with Pcdh18a MO, when both were present in the same aggregates (Figs. 7D–F, I, J, M). A difference in aggregation state between Pcdh18a overexpressing and Pcdh18a depleted cells was supported by quantification of the areas occupied by red and green cells within individual aggregates. The areas were traced, and the ratios for control and experimental aggregates are shown in Fig. 7L. For control cells the ratio is close to unity, but is about half that for experimental cells; the difference is highly significant (see legend of Fig. 7). The data were also evaluated by measuring the largest width and height of red and green cells within the same aggregates, and comparing length and width ratios of control and experimental samples. Again green dimensions were smaller than red dimensions in a highly significant manner (not shown). We conclude that Pcdh18a overexpressing cells sort out from cells in which Pcdh18a expression has been inhibited.

Pcdh18a reduces cell migration within the embryo

In order to further investigate the role of Pcdh18a in cell migration *in vivo* we used cell transplantation. One group of embryos was co-injected with *pcdh18a* RNA and ruby red dextran, while another group was co-injected with *GFP* RNA and fluoro-emerald dextran. Cells from each group were transplanted into an uninjected host at 40% epiboly, delivering both types of cells to the same region of the host (see Materials and methods); embryos were then raised to 80–90% epiboly. Fluorescence photographs taken at the beginning and end of the experiment illustrate a difference in the behavior of the two types of cells such that control (green) cells migrated much farther than cells expressing Pcdh18a (red cells) (Figs. 8A–I). A clear difference, as illustrated in Fig. 8, was seen in 43% of transplanted embryos, while the rest showed similar migration of the two types of cells ($n=54$). Similar results were obtained when transplanting cells injected with UTR-MO or ATG-MO compared to CO-MO-injected cells. The control

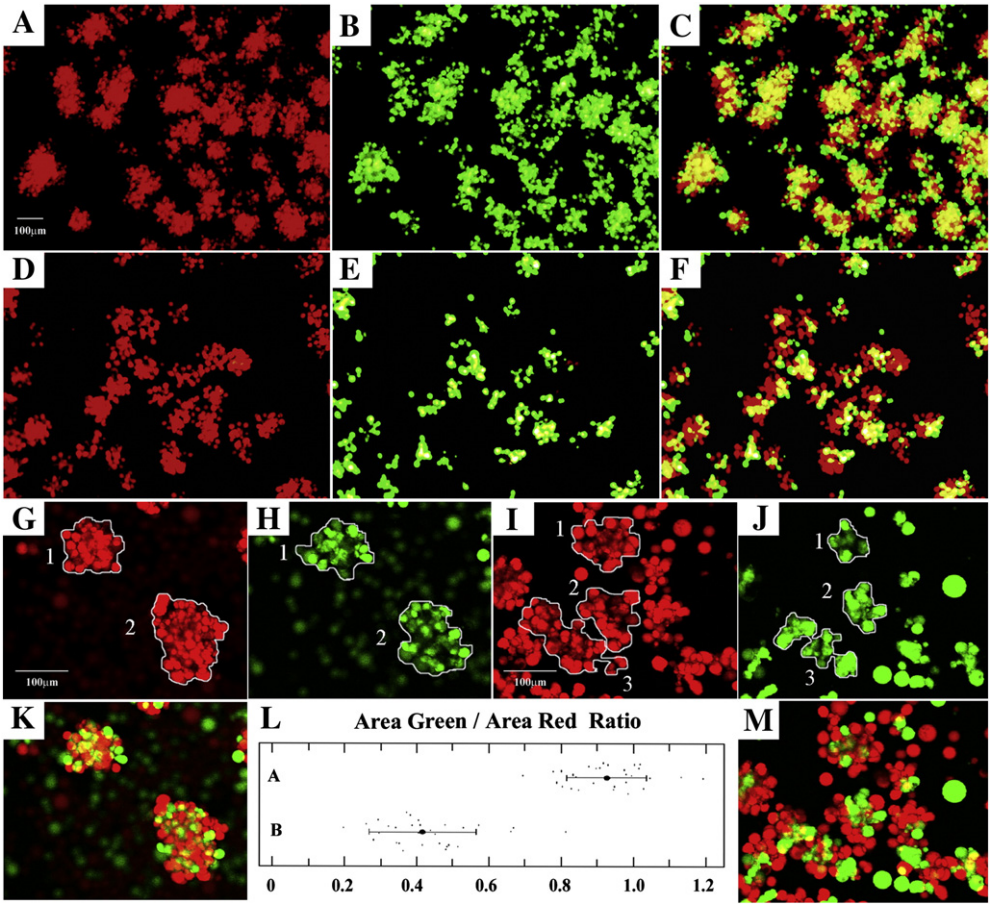

Fig. 7. Pcdh18a affects cell sorting. Red and green labeled cells were mixed and allowed to aggregate (see Materials and methods). Control cells aggregated uniformly (A–C, G, H, K). When red cells injected with pcdh18a 5′ UTR-MO were mixed with green cells injected with *pcdh18a* RNA, aggregates were less uniform with green cells tending to cluster (D–F, I, J, M). To make a quantitative presentation of the effect, we traced the areas occupied by red and green cells in the same aggregate for each of 30 control or experimental aggregates (illustrated in G–J; K, M are merged images), using the "Northern Eclipse" program from Empix Imaging, Inc. (http://empix.com/). The ratios are displayed using the online program (http://www.physics.csbsju.edu/stats/t-test.html) and Microsoft office Excel (L). Panel L shows the control ratios on line A (0.93±0.11) and experimental ratios on line B (0.42±0.15); the difference is highly significant (1.00E−21 by the two tailed *t*-test). Scale bar is 100 μm as shown for panels A–F in panel A, and for panels G–J, K, M in panel G.

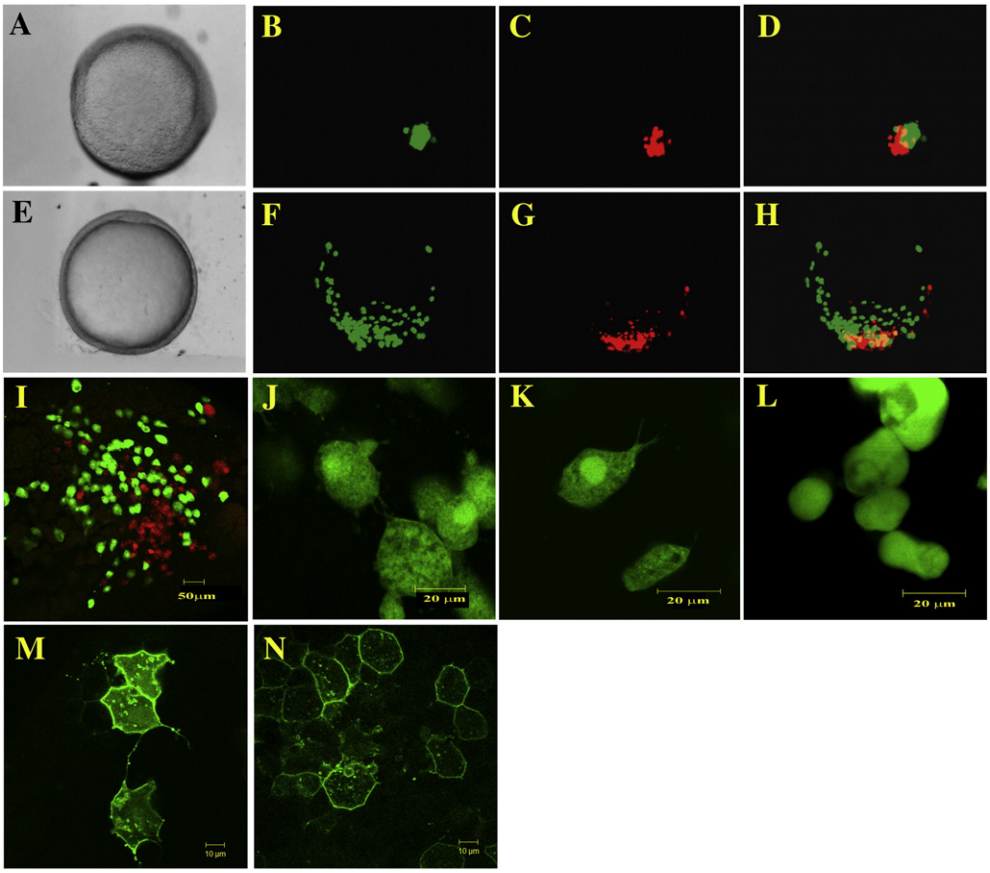

Fig. 8. Cell migration, behavior and shape are affected by Pcdh18a overexpression. Cells from embryos injected with 150–200 pg *GFP* RNA and 2.5 ng fluoro-emerald dextran (green cells), or 150–200 pg *pcdh18a* RNA and 5 ng fluoro-ruby dextran (red cells), were transplanted to the same region in the margin of uninjected host embryos at 40% epiboly (A–D), and cultured to 80–90% epiboly (E–H). Host embryos were examined in visible light (A, E) and by fluorescence microscopy (C, D, F, G; overlays in panels D, H). In 43% of the embryos examined, the green control cells migrated farther than the red Pcdh18a-expressing cells. (I) A different transplanted embryo was examined by confocal microscopy, showing the same effect at higher magnification (scale bar, 50 μm). (J–L) Confocal micrographs of cells from embryos injected with emerald dextran together with 150 pg of *GFP* RNA (J, K), or *pcdh18a* RNA (L), transplanted into separate host embryos. Cell protrusions are visible in control cells but are missing in the *pcdh18a*-expressing cells. Scale bar is 20 μm. Cells shown in panel J are from an embryo fixed and mounted in glycerol, while the cells shown in panels K and L are from live embryos mounted in low melt agarose. (M, N) 20 pg *mGFP* alone or 10 pg *mGFP* in combination with 10 pg *pcdh18a* RNAs was injected into one cell at the 64-cell stage. Confocal microscopy at 70% epiboly showed fewer protrusions in *pcdh18a* RNA-injected embryos compared to controls (M, N). Scale bar in panels M and N is 10 μm.

cells migrated more actively than the test cells which tended to stay closer to each other as a cluster. In three experiments, 64% of the transplanted embryos showed more migration of the control cells compared to UTR-MO-injected test cells (total $n=67$). About 20% showed similar migration, while the rest (16%) showed more migration in the test cells than controls (data not shown). These results suggest that excessive or reduced adhesion inhibits the mobility of cells within the embryo. Further, the effects of an increase or decrease in Pcdh18a expression are cell autonomous as experimental and control cells behave differently in the same unmanipulated host embryo.

Cells overexpressing Pcdh18a show fewer cell protrusions

While observing cells transplanted into host embryos, we noticed that the cell shape differed in the differently-treated cells. Cells overexpressing *pcdh18a* were more regular and have fewer protrusions compared to control *GFP*-injected cells. For improved resolution, transplanted cells were examined by confocal microscopy at the end of the test at 70–80% epiboly. Further, *pcdh18a*-injected and control cells were transplanted into separate hosts, both labeled with fluoro-emerald dextran (green), which afforded better resolution. *GFP*-injected control cells showed numerous, strong protrusions (Figs. 8J, K), whereas cells overexpressing *pcdh18a* were more regular, close to each other, and exhibited no discernable protrusions (Fig. 8L). These results were further supported by injecting *mGFP* alone or in combination with *pcdh18a* RNA into one cell of 64-cell embryos. The embryos were fixed at about 70% epiboly, and labeled cells were observed by confocal microscopy. Once again, the *pcdh18a*-injected cells had a round shape and few membrane protrusions, whereas protrusions were plentiful in control cells (Figs. 8M, N).

Discussion

In the development of a multicellular organism, cell–cell interactions assume a central role. The formation of germ layers and tissues, cell rearrangement and migration, sorting of cells and additional behaviors depend on the cell's ability to recognize its neighbors and other environmental cues. These behaviors are mediated by a variety of components among which the cadherins form a major group of proteins that mediate cell–cell interactions. While the function of classical cadherins is focused on mediating cell–cell adhesion by homophilic interactions, the pcdhs appear to have more varied functions in different developmental stages and tissues. In particular, they have been strongly implicated in early development, and in mammals are particularly abundant in the nervous system with a suggested role in synaptic function (Angst et al., 2001; Bel and Escriche, 2006; Morishita et al., 2006; Suzuki, 2000). Members of the pcdh group can mediate cell–cell adhesion, but they usually contribute weak adhesive forces (Redies et al., 2005). Some evidence

has been generated to suggest that pcdhs have a role in signaling, although such a role is better established for non-classical cadherins in the Flamingo/CELSR group (Takeichi, 2007). The complexity of the pcdh family may contribute to the fact that, in the words of a recent review, "…the protocadherin field is still in its infancy…" (Takeichi, 2007). This complexity has been harnessed through classification into three major groups that are well conserved between human and mouse (Redies et al., 2005). This classification is not always easily applicable to proteins from more distant vertebrates as sequence divergence within this large family can make orthology assignment difficult. For example, sequence analysis cannot decide whether PAPC or PCNS in *Xenopus* is the ortholog of mouse/human Pcdh8 (Rangarajan et al., 2006). In contrast, the zebrafish Pcdh18a protein studied here is much more similar to mammalian Pcdh18 than to any other protein except the zebrafish Pcdh18 paralog reported by Kubota et al. (2008). Notably, the CM1 domain which is only partially conserved among δ2-pcdhs (Vanhalst et al., 2005) is very highly conserved between zebrafish and mammalian Pcdh18 (Supplementary Fig. 1). We are thus confident that the Pcdh18 proteins are orthologs.

Pcdh18a affects cell behavior in the embryo

We have shown that *zfpcdh18a* is expressed widely in the embryo in a discrete pattern, beginning in the dorsal axial region of the gastrula and then most prominently in the early neural ectoderm and forming CNS (Fig. 2). This early and wide expression pattern is consistent with the phenotypic consequences of overexpression and suppression of Pcdh18a in the embryo. The primary consequence is a delay in epiboly and gastrulation movements, leading to disturbed morphogenesis without inhibition of expression of region or cell type-specific genes (Figs. 3–5). This phenotype is comparable to that seen after inhibition of signaling pathways that control convergent extension during gastrulation such as the Wnt–PCP pathway (Heisenberg et al., 2000; Tada et al., 2002; Ulrich et al., 2003). Of particular relevance is the finding of impaired gastrulation movements resulting in short axis and open blastopore after suppression of paraxial pcdh (PAPC) in *Xenopus*, either by direct inhibition of PAPC expression or indirectly via impairment of its upstream regulator Xlim1 (Hukriede et al., 2003; Unterseher et al., 2004). Its name notwithstanding, PAPC is expressed in axial mesoderm in the early gastrula, allowing it to affect the behavior of this tissue at the time when convergent extension initiates. At least part of the activity of PAPC in directing cell movements is mediated by its stimulation of the Wnt–PCP pathway, specifically through activating Rho, Rac and the downstream component c-*jun* N-terminal kinase (JNK) (Unterseher et al., 2004). Manipulating the expression of Pcdh18a similarly affects gastrulation movements in the zebrafish embryo (Figs. 3–5), but it is not known whether these effects are mediated through modulation of a signaling cascade or through the more direct action of Pcdh18a at the cell membrane.

An assembly of phenotypes that includes delayed epiboly, impaired convergent extension and, notably, misplacement of the hatching gland was observed for the *cdh1*^{rk3} mutant, a hypomorphic mutation in the gene that encodes E-cadherin in zebrafish (Shimizu et al., 2005). E-cadherin is a major cell–cell adhesion molecule that is essential for embryonic development in the zebrafish and in the mouse (Larue et al., 1994; Riethmacher et al., 1995). Zebrafish *cdh1*^{rk3} mutant embryos survive to pharyngula stages presumably due to the hypomorphic nature of the mutant allele. It is interesting in the present context that hatching gland migration is a major aspect of the observed phenotype of this mutation (Shimizu et al., 2005).

A role for Pcdh18a in the migration and positioning of hatching gland cells

The precursors of the cells that form the hatching gland are found at the dorsal margin in the early gastrula embryo, interspersed with precursors of the notochord (Kimmel et al., 1990). During gastrulation these cells migrate ahead of the notochord precursors along the AP axis, apparently propelled by both cell migration and cell intercalation behaviors (Daggett et al., 2004), and then form a region named the polster at the anterior edge of the advancing mesoderm. Finally, the hatching gland forms in a ventro-anterior location external to the developing heart, having traversed an unusually long distance by moving from its dorsal origin to a ventral destination. Hatching gland cells are marked by the expression of *hgg1* from the midgastrula onwards, and their correct movements are mediated by the adhesion factor E-cadherin and the actin regulators Quattro and Cap-1 (Daggett et al., 2004; Gardiner et al., 2005; Shimizu et al., 2005), while their differentiation requires the transcriptional regulator Klf4 (Gardiner et al., 2005). In overexpression experiments with Pcdh18a we observed mislocalization of the hatching gland as the most prevalent and most striking phenotype (Fig. 4). Cells expressing *hgg1* remained associated in a contiguous structure, but this structure did not assume the shape or the location of the normal hatching gland. The location of the *hgg1*-positive cells at 24hpf was quite variable within the anterior region of the embryo, but often was ventral or ventro-lateral to the hind- or midbrain (Figs. 4D–H, M–P). These locations are close to the normal location of the hatching gland precursors, the polster, at an earlier stage of development. We surmise that the migration of polster cells initiates more or less normally in Pcdh18a overexpressing embryos, as *hgg1*-positive cells were never found in the trunk or tail region of the embryo, where they would end up if the pre-polster cells were to behave like their neighbors, which are notochord precursors (Kimmel et al., 1990). However, after the end of gastrulation, excess levels of Pcdh18a prevent the progress of polster cells from reaching their destination, leaving them in variable locations along their natural path. This mislocalization of *hgg1*-positive cells is all the more striking as it frequently happens in the context of an essentially normal patterning of the brain. For example, the MHB and rhombomeres 3 and 5, visualized by *eng2* and *krox20*, appear to have formed appropriately in the embryos shown in Figs. 4M–P where *hgg1*-positive cells are found ventral to the anterior hindbrain, far from their normal position. A possible interpretation of these results is that polster cells carry Pcdh18a molecules on their surfaces which, by homophilic interaction with excess Pcdh18a in the environment or through indirect action, slow down their migration in the injected embryos. While the expression pattern of *pcdh18a* does not include the poster, this gene is expressed in dorsal mesoderm in the early gastrula, the region where polster precursors originate (Figs. 2B–E). Other interpretations involving signaling functions of Pcdh18a are possible to explain the differential effect of Pcdh18a overexpression on hatching gland localization.

A role for Pcdh18a in cell–cell adhesion

Pcdhs are believed to be less effective than classical cadherins in mediating cell–cell adhesion, although their extracellular cadherin repeats may be expected to participate in homophilic interactions (Redies et al., 2005; Vanhalst et al., 2005). PAPC, which contributes to cell–cell adhesion and triggers cell sorting, elicits these effects through the regulation of C-cadherin both in *Xenopus* animal caps and in cultured cells (Chen and Gumbiner, 2006). Further, PAPC can trigger the internalization of N-cadherin in synaptic membranes through activation of the p38 MAPK pathway (Yasuda et al., 2007). Our results suggest that Pcdh18a has a role in cellular adhesion, as most explicitly suggested by the dissociation and cell sorting experiments (Figs. 6 and 7). Embryo explants in which Pcdh18a expression was inhibited dissociated faster than control cells when placed in calcium-free medium. While Pcdh18a overexpression did not obviously inhibit dissociation, injection of *pcdh18a* RNA reversed the enhanced dissociation seen in pcdh18a MO-injected explants. Additionally, Pcdh18a overexpressing blastomeres sorted out to a significant extent

from blastomeres injected with pcdh18a UTR-MO. These experiments indicate that Pcdh18a contributes to cell–cell adhesion in blastula cells of the zebrafish embryo, but it remains unknown whether this effect is direct or indirect through intracellular signaling and the regulation of other adhesion molecules.

Experiments testing the role of Pcdh18a on cell movements in vivo also suggest that this molecule affects cell behavior and cell interactions. When transplanted into an uninjected host embryo, cells with increased or reduced Pcdh18a expression showed less migratory activity than control cells. This result is consistent with an adhesive role for Pcdh18a as both excessive and insufficient adhesion can impair cell migration. However, alternative interpretations involving a role of Pcdh18a in signaling could also explain the observed effect. Whichever the cellular basis for the impaired migration, the transplantation experiments are consistent with the mislocalization of the hatching gland after Pcdh18a overexpression, which is an apparent consequence of inhibition of the ventro-anterior migration of the polster cells.

In summary, Pcdh18a is a widely but differentially expressed factor in the zebrafish embryo that has a role in cell–cell adhesion and migration and is essential for normal embryonic development.

Acknowledgment

This research was supported by the Intramural Research Program of the NICHD, National Institutes of Health.

Appendix A. Supplementary data

Supplementary data associated with this article can be found, in the online version, at doi:10.1016/j.ydbio.2008.03.040.

References

Akimenko, M.A., Ekker, M., Wegner, J., Lin, W., Westerfield, M., 1994. Combinatorial expression of three zebrafish genes related to distal-less: part of a homeobox gene code for the head. J. Neurosci. 14, 3475–3486.

Andreas, M., Vogel, T.G., 1997. Expression of a zebrafish *Cathepsin L* gene in anterior mesendoderm and hatching gland. Dev. Genes Evol. 206 (7), 477–479.

Angst, B.D., Marcozzi, C., Magee, A.I., 2001. The cadherin superfamily: diversity in form and function. J. Cell Sci. 114, 629–641.

Bekirov, I.H., Needleman, L.A., Zhang, W., Benson, D.L., 2002. Identification and localization of multiple classic cadherins in developing rat limbic system. Neuroscience 115, 213–227.

Bel, Y., Escriche, B., 2006. Common genomic structure for the Lepidoptera cadherin-like genes. Gene 381, 71–80.

Bradley, R.S., Espeseth, A., Kintner, C., 1998. NF-protocadherin, a novel member of the cadherin superfamily, is required for *Xenopus* ectodermal differentiation. Curr. Biol. 8, 325–334.

Chen, X., Gumbiner, B.M., 2006. Paraxial protocadherin mediates cell sorting and tissue morphogenesis by regulating C-cadherin adhesion activity. J. Cell Biol. 174, 301–313.

Cronin, K.D., Capehart, A.A., 2007. Gamma protocadherin expression in the embryonic chick nervous system. Int. J. Biol. Sci 3, 8–11.

Daggett, D.F., Boyd, C.A., Gautier, P., Bryson-Richardson, R.J., Thisse, C., Thisse, B., Amacher, S.L., Currie, P.D., 2004. Developmentally restricted actin-regulatory molecules control morphogenetic cell movements in the zebrafish gastrula. Curr. Biol. 14, 1632–1638.

Fjose, A., Njolstad, P.R., Nornes, S., Molven, A., Krauss, S., 1992. Structure and early embryonic expression of the zebrafish engrailed-2 gene. Mech. Dev. 39, 51–62.

Frank, M., Kemler, R., 2002. Protocadherins. Curr. Opin. Cell Biol. 14, 557–562.

Furthauer, M., Thisse, C., Thisse, B., 1997. A role for FGF-8 in the dorsoventral patterning of the zebrafish gastrula. Development 124, 4253–4264.

Gardiner, M.R., Daggett, D.F., Zon, L.I., Perkins, A.C., 2005. Zebrafish KLF4 is essential for anterior mesendoderm/pre-polster differentiation and hatching. Dev. Dyn. 234, 992–996.

Gooding, J.M., Yap, K.L., Ikura, M., 2004. The cadherin–catenin complex as a focal point of cell adhesion and signalling: new insights from three-dimensional structures. BioEssays 26, 497–511.

Gurdon, J.B., Brennan, S., Fairman, S., Mohun, T.J., 1984. Transcription of muscle-specific actin genes in early *Xenopus* development: nuclear transplantation and cell dissociation. Cell 38, 691–700.

Hamada, S., Yagi, T., 2001. The cadherin-related neuronal receptor family: a novel diversified cadherin family at the synapse. Neurosci. Res. 41, 207–215.

Heisenberg, C.P., Tada, M., Rauch, G.J., Saude, L., Concha, M.L., Geisler, R., Stemple, D.L., Smith, J.C., Wilson, S.W., 2000. Silberblick/Wnt11 mediates convergent extension movements during zebrafish gastrulation. Nature 405, 76–81.

Hirano, S., Yan, Q., Suzuki, S.T., 1999. Expression of a novel protocadherin, OL-protocadherin, in a subset of functional systems of the developing mouse brain. J. Neurosci 19, 995–1005.

Hirano, S., Suzuki, S.T., Redies, C., 2003. The cadherin superfamily in neural development: diversity, function and interaction with other molecules. Front. Biosci. 8, d306–d355.

Homayouni, R., Rice, D.S., Curran, T., 2001. Disabled-1 interacts with a novel developmentally regulated protocadherin. Biochem. Biophys. Res. Commun. 289, 539–547.

Howell, B.W., Herrick, T.M., Cooper, J.A., 1999. Reelin-induced tyrosine [corrected] phosphorylation of disabled 1 during neuronal positioning. Genes Dev. 13, 643–648.

Howell, B.W., Herrick, T.M., Hildebrand, J.D., Zhang, Y., Cooper, J.A., 2000. Dab1 tyrosine phosphorylation sites relay positional signals during mouse brain development. Curr. Biol. 10, 877–885.

Hukriede, N.A., Tsang, T.E., Habas, R., Khoo, P.L., Steiner, K., Weeks, D.L., Tam, P.P., Dawid, I.B., 2003. Conserved requirement of Lim1 function for cell movements during gastrulation. Dev. Cell 4, 83–94.

Iioka, H., Ueno, N., Kinoshita, N., 2004. Essential role of MARCKS in cortical actin dynamics during gastrulation movements. J. Cell Biol. 164, 169–174.

Kaneko, R., Kato, H., Kawamura, Y., Esumi, S., Hirayama, T., Hirabayashi, T., Yagi, T., 2006. Allelic gene regulation of Pcdh-alpha and Pcdh-gamma clusters involving both monoallelic and biallelic expression in single Purkinje cells. J. Biol. Chem. 281, 30551–30560.

Kim, S.H., Yamamoto, A., Bouwmeester, T., Agius, E., Robertis, E.M., 1998. The role of paraxial protocadherin in selective adhesion and cell movements of the mesoderm during *Xenopus* gastrulation. Development 125, 4681–4690.

Kimmel, C.B., Warga, R.M., Schilling, T.F., 1990. Origin and organization of the zebrafish fate map. Development 108, 581–594.

Kimmel, C.B., Ballard, W.W., Kimmel, S.R., Ullmann, B., Schilling, T.F., 1995. Stages of embryonic development of the zebrafish. Dev. Dyn. 203, 253–310.

Kohmura, N., Senzaki, K., Hamada, S., Kai, N., Yasuda, R., Watanabe, M., Ishii, H., Yasuda, M., Mishina, M., Yagi, T., 1998. Diversity revealed by a novel family of cadherins expressed in neurons at a synaptic complex. Neuron 20, 1137–1151.

Krauss, S., Johansen, T., Korzh, V., Fjose, A., 1991. Expression of the zebrafish paired box gene pax[zf-b] during early neurogenesis. Development 113, 1193–1206.

Kubota, F., Murakami, T., Tajika, Y., Yorifuji, H., 2008. Expression of protocadherin 18 in the CNS and pharyngeal arches of zebrafish embryos. Int. J. Dev. Biol. 52, 2424.

Kudoh, T., Tsang, M., Hukriede, N.A., Chen, X., Dedekian, M., Clarke, C.J., Kiang, A., Schultz, S., Epstein, J.A., Toyama, R., Dawid, I.B., 2001. A gene expression screen in zebrafish embryogenesis. Genome Res. 11, 1979–1987.

Kuroda, H., Inui, M., Sugimoto, K., Hayata, T., Asashima, M., 2002. Axial protocadherin is a mediator of prenotochord cell sorting in *Xenopus*. Dev. Biol. 244, 267–277.

Larue, L., Ohsugi, M., Hirchenhain, J., Kemler, R., 1994. E-cadherin null mutant embryos fail to form a trophectoderm epithelium. Proc. Natl. Acad. Sci. U. S. A. 91, 8263–8267.

Melby, A.E., Kimelman, D., Kimmel, C.B., 1997. Spatial regulation of floating head expression in the developing notochord. Dev. Dyn. 209, 156–165.

Molven, A., Njolstad, P.R., Fjose, A., 1991. Genomic structure and restricted neural expression of the zebrafish wnt-1 (int-1) gene. EMBO J. 10, 799–807.

Morishita, H., Umitsu, M., Murata, Y., Shibata, N., Udaka, K., Higuchi, Y., Akutsu, H., Yamaguchi, T., Yagi, T., Ikegami, T., 2006. Structure of the cadherin-related neuronal receptor/protocadherin-alpha first extracellular cadherin domain reveals diversity across cadherin families. J. Biol. Chem. 281, 33650–33663.

Munton, R.P., Vizi, S., Mansuy, I.M., 2004. The role of protein phosphatase-1 in the modulation of synaptic and structural plasticity. FEBS Lett. 567, 121–128.

Nagar, B., Overduin, M., Ikura, M., Rini, J.M., 1996. Structural basis of calcium-induced E-cadherin rigidification and dimerization. Nature 380, 360–364.

Nollet, F., Kools, P., van Roy, F., 2000. Phylogenetic analysis of the cadherin superfamily allows identification of six major subfamilies besides several solitary members. J. Mol. Biol. 299, 551–572.

Oxtoby, E., Jowett, T., 1993. Cloning of the zebrafish krox-20 gene (krx-20) and its expression during hindbrain development. Nucleic Acids Res. 21, 1087–1095.

Patel, S.D., Chen, C.P., Bahna, F., Honig, B., Shapiro, L., 2003. Cadherin-mediated cell–cell adhesion: sticking together as a family. Curr. Opin. Struct. Biol. 13, 690–698.

Pfeffer, P.L., Gerster, T., Lun, K., Brand, M., Busslinger, M., 1998. Characterization of three novel members of the zebrafish Pax2/5/8 family: dependency of Pax5 and Pax8 expression on the Pax2.1 (noi) function. Development 125, 3063–3074.

Rangarajan, J., Luo, T., Sargent, T.D., 2006. PCNS: a novel protocadherin required for cranial neural crest migration and somite morphogenesis in *Xenopus*. Dev. Biol. 295, 206–218.

Redies, C., 2000. Cadherins in the central nervous system. Prog. Neurobiol. 61, 611–648.

Redies, C., Vanhalst, K., Roy, F., 2005. delta-Protocadherins: unique structures and functions. Cell Mol. Life Sci. 62, 2840–2852.

Reifers, F., Bohli, H., Walsh, E.C., Crossley, P.H., Stainier, D.Y., Brand, M., 1998. Fgf8 is mutated in zebrafish acerebellar (ace) mutants and is required for maintenance of midbrain–hindbrain boundary development and somitogenesis. Development 125, 2381–2395.

Reiss, K., Maretzky, T., Haas, I.G., Schulte, M., Ludwig, A., Frank, M., Saftig, P., 2006. Regulated ADAM10-dependent ectodomain shedding of gamma-protocadherin C3 modulates cell–cell adhesion. J. Biol. Chem. 281, 21735–21744.

Riethmacher, D., Brinkmann, V., Birchmeier, C., 1995. A targeted mutation in the mouse E-cadherin gene results in defective preimplantation development. Proc. Natl. Acad. Sci. U. S. A. 92, 855–859.

Sano, K., Tanihara, H., Heimark, R.L., Obata, S., Davidson, M., St John, T., Taketani, S., Suzuki, S., 1993. Protocadherins: a large family of cadherin-related molecules in central nervous system. EMBO J. 12, 2249–2256.

Sargent, T.D., Jamrich, M., Dawid, I.B., 1986. Cell interactions and the control of gene activity during early development of *Xenopus laevis*. Dev. Biol. 114, 238–246.
Schulte-Merker, S., van Eeden, F.J., Halpern, M.E., Kimmel, C.B., Nusslein-Volhard, C., 1994. no tail (ntl) is the zebrafish homologue of the mouse T (Brachyury) gene. Development 120, 1009–1015.
Shapiro, L., Colman, D.R., 1999. The diversity of cadherins and implications for a synaptic adhesive code in the CNS. Neuron 23, 427–430.
Shapiro, L., Fannon, A.M., Kwong, P.D., Thompson, A., Lehmann, M.S., Grubel, G., Legrand, J.F., Als-Nielsen, J., Colman, D.R., Hendrickson, W.A., 1995. Structural basis of cell–cell adhesion by cadherins. Nature 374, 327–337.
Shimizu, T., Yabe, T., Muraoka, O., Yonemura, S., Aramaki, S., Hatta, K., Bae, Y.K., Nojima, H., Hibi, M., 2005. E-cadherin is required for gastrulation cell movements in zebrafish. Mech. Dev. 122, 747–763.
Suzuki, S.T., 2000. Recent progress in protocadherin research. Exp. Cell Res. 261, 13–18.
Tada, M., Concha, M.L., Heisenberg, C.P., 2002. Non-canonical Wnt signalling and regulation of gastrulation movements. Semin. Cell Dev. Biol. 13, 251–260.
Takeichi, M., 1991. Cadherin cell adhesion receptors as a morphogenetic regulator. Science 251, 1451–1455.
Takeichi, M., 1988. The cadherins: cell–cell adhesion molecules controlling animal morphogenesis. Development 102, 639–655.
Takeichi, M., 2007. The cadherin superfamily in neuronal connections and interactions. Nat. Rev., Neurosci. 8, 11–20.
Tepass, U., Truong, K., Godt, D., Ikura, M., Peifer, M., 2000. Cadherins in embryonic and neural morphogenesis. Nat. Rev., Mol. Cell Biol. 1, 91–100.
Thisse, C., Thisse, B., Halpern, M.E., Postlethwait, J.H., 1994. Goosecoid expression in neurectoderm and mesendoderm is disrupted in zebrafish cyclops gastrulas. Dev. Biol. 164, 420–429.
Turner, D.L., Weintraub, H., 1994. Expression of achaete–scute homolog 3 in *Xenopus* embryos converts ectodermal cells to a neural fate. Genes Dev. 8, 1434–1447.
Uemura, T., 1998. The cadherin superfamily at the synapse: more members, more missions. Cell 93, 1095–1098.
Ulrich, F., Concha, M.L., Heid, P.J., Voss, E., Witzel, S., Roehl, H., Tada, M., Wilson, S.W., Adams, R.J., Soll, D.R., Heisenberg, C.P., 2003. Slb/Wnt11 controls hypoblast cell migration and morphogenesis at the onset of zebrafish gastrulation. Development 130, 5375–5384.
Unterseher, F., Hefele, J.A., Giehl, K., De Robertis, E.M., Wedlich, D., Schambony, A., 2004. Paraxial protocadherin coordinates cell polarity during convergent extension via Rho A and JNK. EMBo J. 23, 3259–3269.
Vanhalst, K., Kools, P., Staes, K., van Roy, F., Redies, C., 2005. delta-Protocadherins: a gene family expressed differentially in the mouse brain. Cell Mol. Life Sci. 62, 1247–1259.
Vleminckx, K., Kemler, R., 1999. Cadherins and tissue formation: integrating adhesion and signaling. BioEssays 21, 211–220.
Westerfield, M., 2000. THE ZEBRAFISH BOOK; A guide for the laboratory use of zebrafish (*Danio rerio*). University of Oregon Press, Eugene, OR.
Wheelock, M.J., Johnson, K.R., 2003. Cadherins as modulators of cellular phenotype. Annu. Rev. Cell Dev. Biol. 19, 207–235.
Wolverton, T., Lalande, M., 2001. Identification and characterization of three members of a novel subclass of protocadherins. Genomics 76, 66–72.
Wu, Q., Maniatis, T., 2000. Large exons encoding multiple ectodomains are a characteristic feature of protocadherin genes. Proc. Natl. Acad. Sci. U. S. A. 97, 3124–3129.
Yagi, T., Takeichi, M., 2000. Cadherin superfamily genes: functions, genomic organization, and neurologic diversity. Genes Dev. 14, 1169–1180.
Yamagata, K., Andreasson, K.I., Sugiura, H., Maru, E., Dominique, M., Irie, Y., Miki, N., Hayashi, Y., Yoshioka, M., Kaneko, K., Kato, H., Worley, P.F., 1999. Arcadlin is a neural activity-regulated cadherin involved in long term potentiation. J. Biol. Chem. 274, 19473–111979.
Yasuda, S., Tanaka, H., Sugiura, H., Okamura, K., Sakaguchi, T., Tran, U., Takemiya, T., Mizoguchi, A., Yagita, Y., Sakurai, T., De Robertis, E.M., Yamagata, K., 2007. Activity-induced protocadherin arcadlin regulates dendritic spine number by triggering N-cadherin endocytosis via TAO2beta and p38 MAP kinases. Neuron 56, 456–471.
Yoshida, K., 2003. Fibroblast cell shape and adhesion in vitro is altered by overexpression of the 7a and 7b isoforms of protocadherin 7, but not the 7c isoform. Cell Mol. Biol. Lett. 8, 735–741.
Yoshida, K., Watanabe, M., Kato, H., Dutta, A., Sugano, S., 1999. BH-protocadherin-c, a member of the cadherin superfamily, interacts with protein phosphatase 1 alpha through its intracellular domain. FEBS Lett. 460, 93–98.
Zou, C., Huang, W., Ying, G., Wu, Q., 2007. Sequence analysis and expression mapping of the rat clustered protocadherin gene repertoires. Neuroscience 144, 579–603.